

# Weighting Factor Design for FS-MPC in VSCs: A Brain Emotional Learning-Based Approach

Mohammad Sadegh Orfi Yeganeh  
Technical University of Denmark  
2800 Kgs. Lyngby, Denmark  
morfi@dtu.dk

Arman Oshnoci  
Aalborg University  
Aalborg, Denmark  
aros@et.aau.dk

Saeed Peyghami  
Aalborg University  
Aalborg, Denmark  
sap@energy.aau.dk

Nenad Mijatovic  
Technical University of Denmark  
2800 Kgs. Lyngby, Denmark  
nm@dtu.dk

Tomislav Dragicevic  
Technical University of Denmark  
2800 Kgs. Lyngby, Denmark  
tomdr@dtu.dk

Frede Blaabjerg  
Aalborg University  
Aalborg, Denmark  
fbl@energy.aau.dk

## Keywords

Brain emotional learning (BEL) - Finite set model predictive control (FS-MPC) - Total harmonic distortion (THD) - Uninterruptible power supply (UPS).

## Abstract

Finite set model predictive control (FS-MPC) has been identified as one of the most favorable controllers for power electronic applications due to its capability over real-time solutions to multiple objectives and constraints. However, the main challenge in the FS-MPC is the choice of appropriate weighting factors in the cost function to reach the best switching state of the inverter. This study proposes an approach based on brain emotional learning (BEL) to provide online tuning of weighting factors in FS-MPC of a power converter, which prevents the dependency of the converter control system on the various uncertainties coming from operating conditions and loading conditions. The proposed BEL approach is fully model-free, indicating that the weighting factors are adjusted without previous knowledge of the system model and parameters. Simulation and experimental results validate the proposed control scheme's effectiveness under different load conditions.

## 1. Introduction

Among different converter topologies, voltage source converters (VSCs) are the most widely spread in practice. Many advanced control techniques and topologies for VSCs have been proposed over the past years, aiming to mitigate some of the well-known limitations of classical linear control approaches [1] and [2]. Power converters and motor drives play an important role in power electronics technology and various industrial applications such as renewable energy sources, electric vehicles, HVDC transmission systems, and uninterrupted power supply systems (UPS).

Finite control set model predictive control (FS-MPC) has been extensively utilized in both academia and industry in the last decades. This control method bears many advantages such as there is no need for a modulation stage, constraints can be included in the main cost function, the easy inclusion of non-linearities in the model, and low complexity that makes the implementation much easier. In contrary to the conventional control techniques, the FS-MPC is capable of obtaining faster dynamic response and higher frequency bandwidth [3-5].

The performance of FS-MPC is deeply influenced by the weighting factors, the tuning of which is still a challenge to be undertaken [6]. Recently, model-free intelligent controllers such as fuzzy logic and neural network have been developed to decrease the sensitivity to modeling inaccuracy. The main characteristic of intelligent controllers is the model-free design that enables them to manage model non-linearity, complexity, and uncertainty in power electronic applications [7]. In this regard, refs. [8] and [9] have employed an artificial neural network method in the off-line mode for weighting factor design of FS-MPC in UPS and motor drives applications. This method, however, demands many computations to cover all the assortments of the possible coefficients. Also, the conducted analysis for identifying the

optimal values of weighting factors is dependent on operating conditions, which may give rise to a flawed performance of the control system. A model based on the emotional learning in the human brain's limbic system was developed in [10]. The brain emotional learning (BEL) model is an effective controller for fast decision-making, particularly in uncertain states. The online learning capacity, minimum computational intricacy, and, most notably, no demand for prior knowledge of system dynamics make the BEL a distinctive controller over other intelligent controllers. Also, it is simple, with fewer tuning parameters in emotional controllers, and it does not need a further iterative procedure for updating parameters or learning [11]. The BEL is growingly being utilized in electrical motors [12], control engineering [13], and intelligent devices [14]. It is illustrated in [10] that the BEL can present more effective solutions than neural networks and fuzzy logic in controlling the synchronous machines in power systems.

Motivated by the previous discussion, this paper proposes a model-free and adaptive approach based on BEL to adjust the weighting factors appearing in the FS-MPC objective function. The proposed BEL-based FS-MPC is applied to a benchmark UPS VSC system. The proposed strategy is totally model-free, suggesting that the weighting factors are tuned without previous knowledge of the parameters and system model. The method offers superior performance in varying operating point conditions. To achieve optimum results with the BEL method working based on the knowledge of the experts, considering desirable scaling factors are the necessary part, which is also addressed in this paper. Both simulation and experimental validations are provided to demonstrate the effectiveness of the proposed control scheme.

## 2. Finite set model predictive control principle

In this paper, a BEL-based FS-MPC approach is proposed to adjust the voltage and current of the VSC, and reduce the switching losses. Fig. 1 illustrates the BEL-based FS-MPC that is operated on a VSC for UPS application. In this way, a proper control command is obtained based on the prediction from the converter model and a cost objective function. The converter model is a two-level three-phase VSC, in which there are eight switching states in total.

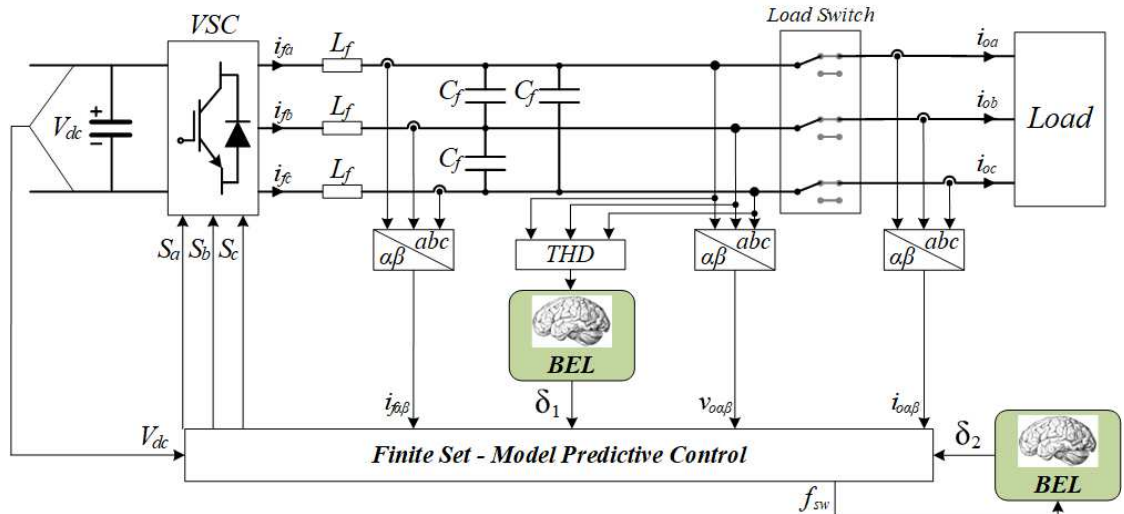


Fig. 1: A schematic of the proposed control structure and power section

To eliminate the harmonics of the output voltage and current, a three-phase LC filter is connected to the load (see Fig. 1).  $R_f$ ,  $C_f$ , and  $L_f$  are the resistance, capacitance, and inductance of the LC filter, respectively. The output current ( $i_o$ ), the filter current ( $i_f$ ), and output voltage ( $v_o$ ) are presented in vectors as follows:

$$i_o = [i_{ou} \quad i_{ov} \quad i_{ow}]^T \quad (1)$$

$$i_f = [i_{fu} \quad i_{fv} \quad i_{fw}]^T \quad (2)$$

$$v_o = [v_{ou} \quad v_{ov} \quad v_{ow}]^T \quad (3)$$

Three-phase variable vectors are transferred to a two-dimensional vector ( $\alpha\beta$  stationary reference frame) by employing the Clarke transformation (T) as follows:

$$T = 1/3 \begin{bmatrix} 1 & e^{j\frac{2}{3}\pi} & e^{j\frac{4}{3}\pi} \end{bmatrix} \quad (4)$$

Finally, the output voltage and current of the converter can be expressed in the state-space form as follows:

$$\frac{d}{dt} \begin{bmatrix} i_f \\ v_f \end{bmatrix} = A \begin{bmatrix} i_f \\ v_f \end{bmatrix} + B \begin{bmatrix} v_i \end{bmatrix} \quad (5)$$

$$A = \begin{bmatrix} -\frac{R_f}{L_f} & -\frac{1}{L_f} \\ \frac{1}{C_f} & 0 \end{bmatrix} \quad (6)$$

$$B = \begin{bmatrix} \frac{1}{L_f} & 0 \\ 0 & -\frac{1}{C_f} \end{bmatrix} \quad (7)$$

where  $A$  is the system matrix,  $B$  is the control matrix, and  $v_i$  is the input voltage.

The MPC control technique works based on predicting  $v_f$  and  $i_f$ , and then applying a proper magnitude for  $v_i$  in the objective function. Therefore, the main objective function consists of the prediction error ( $v_e$ ) with a weighting factor ( $\delta_1$ ), the current limitation ( $\varepsilon_{lim}$ ), the number of switching efforts ( $SW$ ) with a weighting factor ( $\delta_2$ ), and a minimizer for the voltage derivative ( $v_{reg}$ ), which is given as below

$$v_e(k) = v_f(k+1) - v_{ref}(k) \quad (8)$$

$$\varepsilon_{lim}(k) = \begin{cases} 0, & \text{if } |i_f(k)| \leq i_{max} \\ \infty, & \text{if } |i_f(k)| > i_{max} \end{cases} \quad (9)$$

$$SW(k) = \sum |u(k) - u(k-1)| \quad (10)$$

$$v_{reg}(k) = (C_f \cdot w_{ref} \cdot v_{f\beta}(k+1) - i_{f\alpha} + i_{o\alpha})^2 + (C_f \cdot w_{ref} \cdot v_{f\alpha}(k+1) - i_{f\alpha} + i_{o\beta})^2 \quad (11)$$

$$\text{CF: } \delta_1 \cdot v_e(k) + \varepsilon_{lim}(k) + \delta_2 \cdot SW(k) + v_{reg}(k) \quad (12)$$

$$f_{sw} = \sum_{k=1}^{1/T_s} \frac{|\Delta S_a(k)| + |\Delta S_b(k)| + |\Delta S_c(k)|}{6} \quad (13)$$

where  $v_{ref}$  and  $w_{ref}$  are the voltage and frequency of the reference signal, respectively. As it can be seen, the system performance is highly influenced by the weighting factors ( $\delta_1$  and  $\delta_2$ ), which should be adjusted optimally. In this paper, the BEL method is proposed to adjust the weighting factors and thereby improve the performance of the converter control system. Performance evaluation criteria include the converter's switching frequency and the total harmonic distortion (THD) of the output voltage. The design process of the BEL-based regulation scheme is discussed in the next section.

### 3. BEL-based regulation scheme

The BEL is used as a model-free method in a range of control engineering applications. The BEL can learn quick-auto, and thus it is proper for robust and fast decision-making in nonlinear systems, especially in systems with uncertainty. In [15], the BEL controller has superior performance compared with PI and fuzzy logic controllers in both online and offline simulations for PMSM drive systems in different test conditions. This method is constituted by the Amygdala, which is in charge of emotional learning; the orbitofrontal cortex, sensory cortex, and Thalamus [10]. The model is provided with two inputs including sensory input (*SI*) and emotional signal (*ES*). Preprocessing of *SI* signals such as filtering or noise reduction is performed by the Thalamus. The sensory cortex receives the Thalamus output and then submits it to the Amygdala and Orbitofrontal cortex. A simplified structure of the BEL used in this work is depicted in Fig. 2. *A* and *O* networks, respectively, express the functional blocks associated with the amygdala and orbitofrontal cortex. The BEL output is obtained based on the subtraction of network *A* and network *O* outputs as follows.

$$M = \sum_z A_z - \sum_z O_z \quad (14)$$

The output of *A* network is computed as

$$A_{th} = \max(S_z) \quad (15)$$

$$A_z = S_z G_z \quad (16)$$

where  $A_{th}$  is a neuron that receives maximum sensory signals from the thalamus directly. Similarly, the output of the OC network is given by:

$$O_z = S_z H_z \quad (17)$$

The weights in AD and OC networks are updated by using (18) and (19)

$$\Delta G_z = \alpha [S_z \max(0, ES - \sum_z A_z)] \quad (18)$$

$$\Delta H_z = \gamma [S_z (\sum_z O_z - ES)] \quad (19)$$

where  $\alpha$  and  $\gamma$  are BEL's learning rates. The schematic diagram of the proposed BEL-based regulation scheme is depicted in Fig. 3. The critical functionality of this structure is to minimize the THD and switching frequency. The BEL output is supplementary regulation coefficients to update the weighting factors of the FC-MPC. This adaptive feature improves the converter's robustness against different uncertainties and a vast range of working states. Since the FS-MPC includes two weighting factors, thus two BEL structures are designed. To attain favorable performance of the BEL-based approach, constituting an empirical relation between *SI*, *ES*, and output ( $\delta_1$  and  $\delta_2$ ) is essential. The *SI* and *ES* inputs for the first BEL to find the optimal value of  $\delta_1$  are (20) and (21), respectively.

$$SI = \mu_1 THD + \mu_2 \int THD dt \quad (20)$$

$$ES = \mu_3 THD + \mu_4 \int THD dt + \mu_4 \delta_1 \quad (21)$$

Similarly, for the second BEL to find the optimal value of  $\delta_2$ , the *SI* and *ES* inputs are written as follows:

$$SI = \lambda_1 f_{sw} + \lambda_2 \int f_{sw} dt \quad (22)$$

$$ES = \lambda_3 f_{sw} + \lambda_4 \int f_{sw} dt + \lambda_4 \delta_1 \quad (23)$$

The weighting coefficients appearing in (20), (21), (22), and (23) are determined through a trial and error process by simulations. The functions *SI* and *ES* are chosen as the outputs of a PI block in response

to the THD and  $f_{sw}$  signals. In other words, those weights are the same as proportional and integral coefficients appearing in the PI controller.

Two scaling coefficients (SCs) are added to the coordinator body to normalize the outputs. A particle swarm optimization algorithm tunes the SCs by minimizing the following performance index.

Performance index:

$$\min F = \int_{t=0}^{T_s} t(\Delta v_o^2) dt \quad (24)$$

Decision variables:

$$SF_{Ai,min} \leq SF_{Ai} \leq SF_{Ai,max} \quad (25)$$

$$SF_{Pi,min} \leq SF_{Pi} \leq SF_{Pi,max} \quad (26)$$

where  $\Delta v_o$  represents the output voltage deviation; and  $T_s$  is the time length of  $\Delta v_o$ . As (24) implies, the integral of time multiplied by squared error (ITSE) is used to obtain the optimal solution.

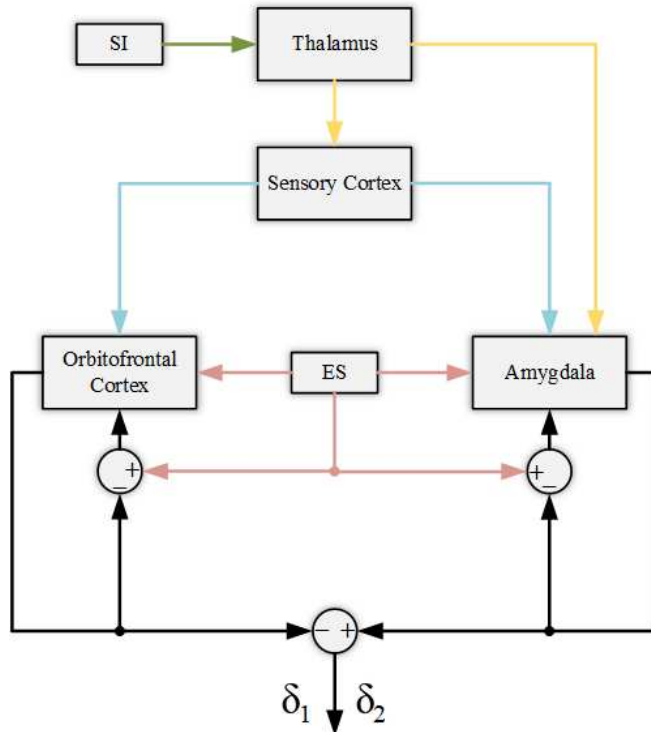


Fig. 2: Structure of BEL approach

#### 4. Simulation and experimental results

The proposed weighting factor design strategy has been verified experimentally with a test system. As mentioned in Fig. 1, the experimental setup consists of a full-bridge three-phase VSC (SEMITEACH IGBT, 20kW), and a DC power supply (Delta Elektronika SM1500-CP-30), an LC filter, impedances, measurements, and resistive loads are employed and illustrated in Fig. 3. In addition, a dSpace MicroLab Box DS-1202 is used in the control section. Details of the utilized parameters are provided in Table I.

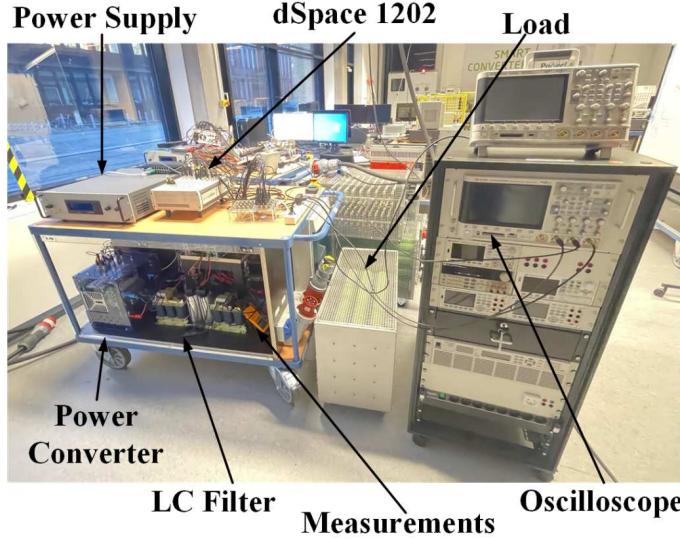


Fig. 3: A photograph of the experimental motor drive test setup

**Table I. Parameters of the test system**

Component Parameters		
Parameters	Symbol	Value
DC power supply	$V_{dc}$	260 V
Nominal voltage magnitude	$V_{ref}$	100 V
Nominal frequency	$f_{ref}$	50 Hz
Sampling time	$T_s$	25 $\mu$ s
Capacitance of LC filter	$C_f$	10 $\mu$ F
Inductance of LC filter	$L_f$	2.2 mH
Load 1	$R_{Load1}$	58 $\Omega$
Load 2	$R_{Load2}$	116 $\Omega$
Load 3	$R_{Load3}$	12 $\Omega$

Control Parameters		
	$\alpha$	$\beta$
Switching Frequency Section (BEL Parameters)	2	-1
THD Section (BEL Parameters)	1	1

Based on standard (IEC 62040-3), the UPS should follow different tests on performance, components, and main parts [16]. To verify the dynamic performance of the proposed control technique, a two-step load change has been carried out on the UPS setup. Therefore, the controller has been tested for three different resistive loads. In this way, for the first test, at  $t = 2.0$  s, load 1 ( $58 \Omega$ ) is paralleled with load 2 ( $116 \Omega$ ), thus the equal resistance is around  $39 \Omega$ . According to Fig. 4 (a), the FS-MPC controller can perform properly and control the voltage magnitude by well tracking the reference value. The current waveform is presented in Fig. 4 (b), and it has been increased due to impedance reduction on the load side. Fig. 4 (a) and (b) present a fast and proper performance of the proposed control strategy. The magnitudes of THD and switching frequency of the proposed control technique are improved by utilizing the BEL controller, which can be seen in a comparison with Table III in [9]. Another

achievement of the proposed solution of this study is designing the weighting factors in an online approach, which can overcome the defects of the state-of-the-art ([8] and [9]). Based on Fig. 4 (c) and (d), the optimal value of the switching frequency and THD magnitudes are floating and they are around 6.3 kHz and 1.2% respectively. By utilizing the mentioned values of the control parameters in Table I, the weighting factors of the cost functions for the switching frequency and THD are obtained and presented in Fig. 4 (e) and (f). The value of the switching frequency weighting factor is around 4.8 most of the time, and the value of the THD weighting factor has a variation around 1.1.

For the second test, at  $t = 2.0$  s, load 3 ( $12 \Omega$ ) is paralleled with load 2 ( $116 \Omega$ ), thus the equal resistance is around  $11 \Omega$ . According to Fig. 5 (a) and (b), the FS-MPC controller can perform properly and control the voltage and current by employing the BEL controller for the weighting factor design. In this test, the load variations are higher than in the first test, so there are more changes in both weighting factors at  $t = 2.0$  s in comparison with the previous test. The figures also reveal that the BEL-based method regulates the weighting coefficients such that a stable operation of the VSC is achieved.

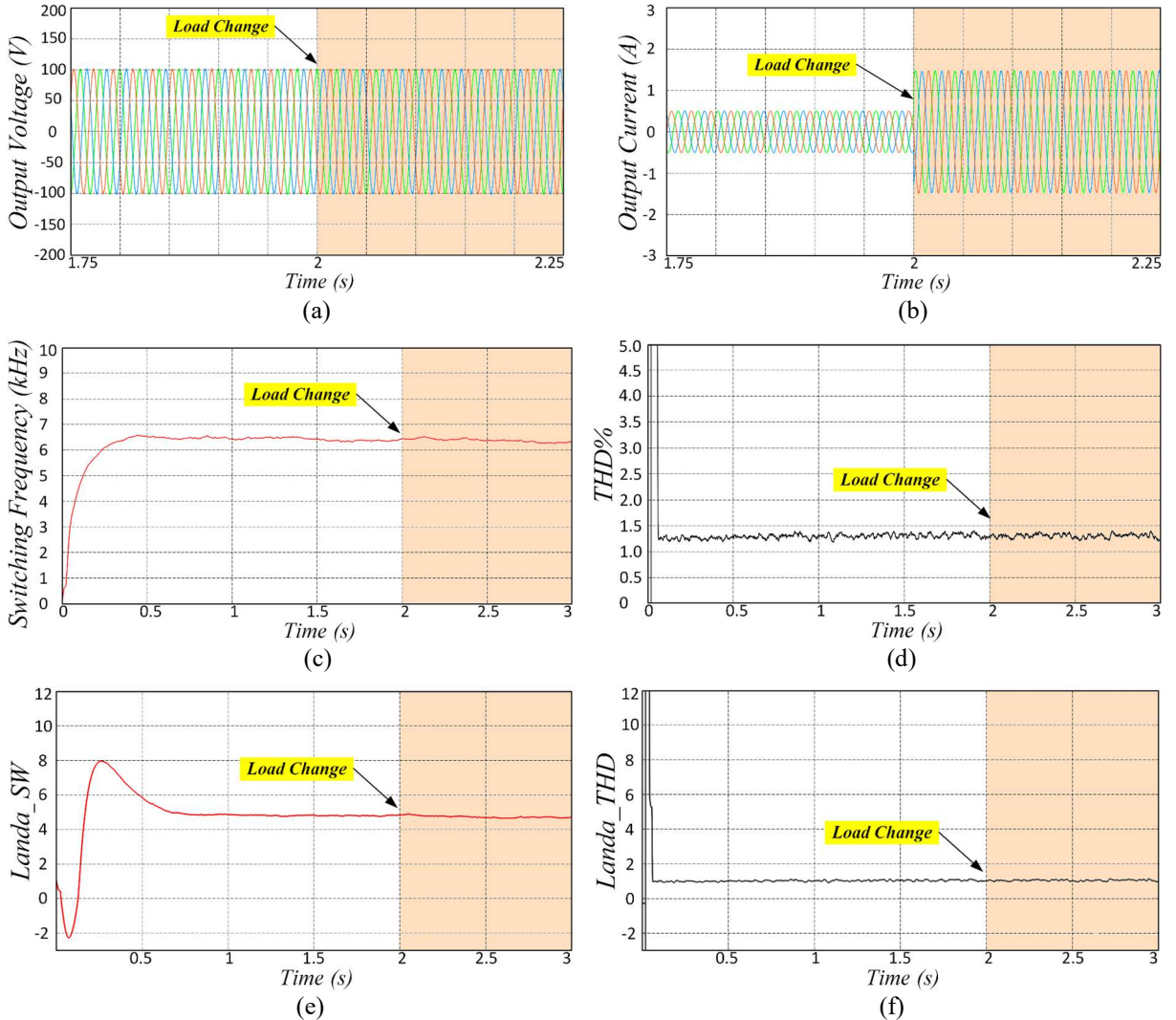


Fig. 4: Simulation results of the specified first test, (a) Output voltage, (b) Output current, (c) Switching frequency, (d) Total harmonic distortion of the output voltage, (e) Switching frequency weighting factor ( $\delta_1$ ), and (f) THD weighting factor ( $\delta_2$ )

The proposed control strategy's robust and optimal design of the weighting factors has been demonstrated experimentally for the first test in Fig. 6 (a) and (b). The experimental results of the power converter's output voltage and current validate the obtained simulation results.

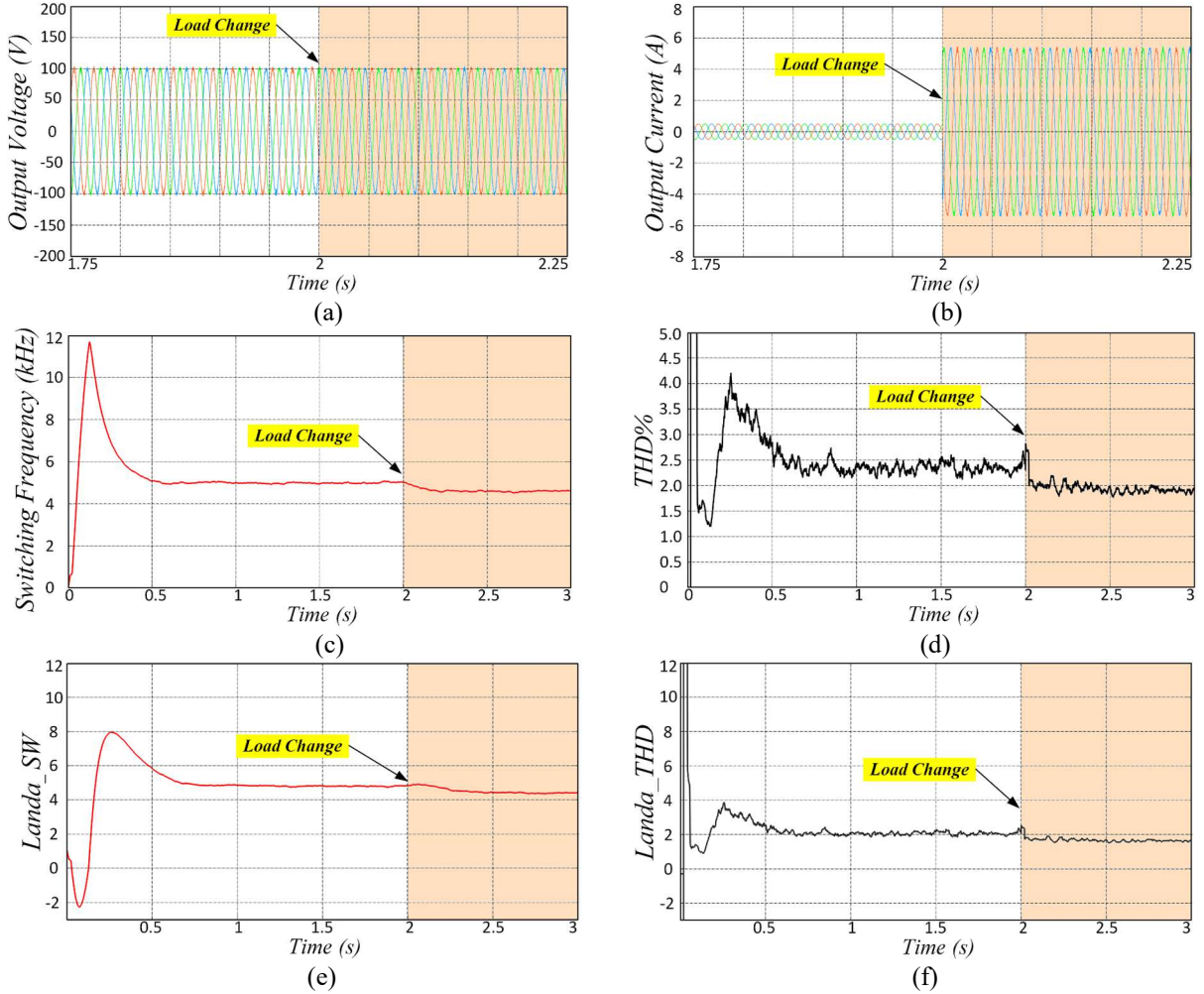


Fig. 5: Simulation results of the specified second test, (a) Output voltage, (b) Output current, (c) Switching frequency, (d) Total harmonic distortion of the output voltage, (e) Switching frequency weighting factor ( $\delta_1$ ), and (f) THD weighting factor ( $\delta_2$ ).

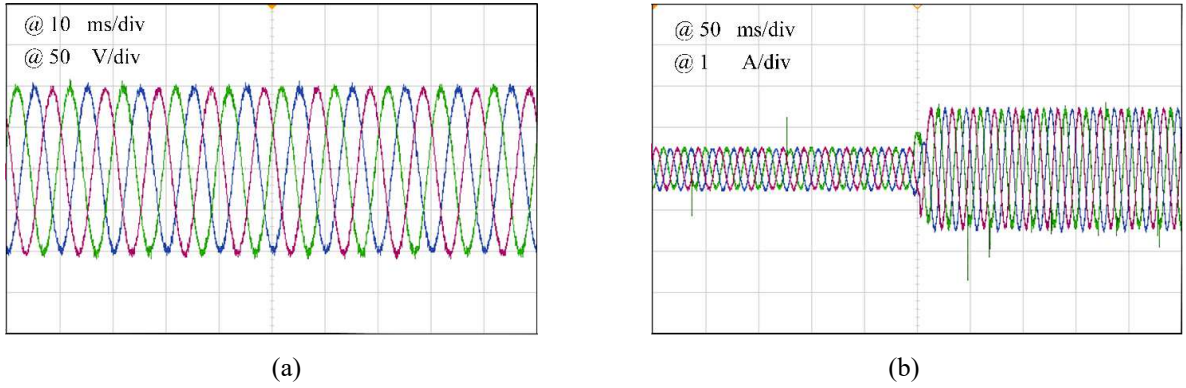


Fig. 6: Experimental results of the specified first test, (a) Output voltage, and (b) Output current of the power converter

## Conclusion

In this study, a real-time solution by employing brain emotional learning method was proposed to design the weighting factors of the FS-MPC. The approach's effectiveness was illustrated on a UPS VSC setup. Minimizing the switching frequency and THD were the main objectives behind the BEL-based FS-MPC method. The proposed method's key features are the online learning capacity, minimum computational

complexity, and there is no need for prior knowledge of the VSC dynamics. Finally, the simulation and experimental results demonstrated the effectiveness of the proposed strategy under different operational conditions.

## References

- [1] Yeganeh, M.S.O., Davari, P., Chub, A., Mijatovic, N., Dragicevic, T. and Blaabjerg, F., "A Single-Phase Reduced Component Count Asymmetrical Multilevel Inverter Topology," IEEE Journal of Emerging and Selected Topics in Power Electronics, 9(6), pp.6780-6790, 2021.
- [2] Heydari, R., Khayat, Y., Amiri, A., Dragicevic, T., Shafiee, Q., Popovski, P. and Blaabjerg, F., "Robust high-rate secondary control of microgrids with mitigation of communication impairments," IEEE Transactions on Power Electronics, 35(11), pp.12486-12496, 2020.
- [3] Khayat, Y., Heydari, R., Naderi, M., Dragicevic, T., Shafiee, Q., Fathi, M., Bevrani, H. and Blaabjerg, F., "Decentralized frequency control of AC microgrids: an estimation-based consensus approach," IEEE Journal of Emerging and Selected Topics in Power Electronics, 9(5), pp.5183-5191, 2020.
- [4] Yeganeh, M.S.O., Mijatovic, N. and Dragicevic, T., "Dynamic Performance Optimization of Single-Phase Inverter based on Model Predictive Control," In 2021 IEEE International Conference on Predictive Control of Electrical Drives and Power Electronics (PRECEDE) (pp. 235-240). IEEE, 2021.
- [5] Mardani, M.M., Mijatovic, N. and Dragicevic, T., "Optimal Model Predictive Controller for Grid-Connected Voltage Source Converters," In 31st IEEE International Symposium on Industrial Electronics. IEEE., 2021.
- [6] Ding, D., Yeganeh, M.S.O., Mijatovic, N., Wang, G. and Dragicevic, T., "Model Predictive Control on Three-Phase Converter for PMSM Drives with a Small DC-link Capacitor," In 2021 IEEE International Conference on Predictive Control of Electrical Drives and Power Electronics (PRECEDE) (pp. 224-228). IEEE, 2021.
- [7] Oshnoei, A., Sadeghian, O., Mohammadi-Ivatloo, B., Blaabjerg, F. and Anvari-Moghaddam, A., "Data-Driven Coordinated Control of AVR and PSS in Power Systems: A Deep Reinforcement Learning Method," In 2021 IEEE International Conference on Environment and Electrical Engineering and 2021 IEEE Industrial and Commercial Power Systems Europe (EEEIC/I&CPS Europe) (pp. 1-6). IEEE, 2021.
- [8] Novak, M., Xie, H., Dragicevic, T., Wang, F., Rodriguez, J. and Blaabjerg, F., "Optimal cost function parameter design in predictive torque control (PTC) using artificial neural networks (ANN)," IEEE Transactions on Industrial Electronics, 68(8), pp.7309-7319, 2020.
- [9] Dragičević, T. and Novak, M., "Weighting factor design in model predictive control of power electronic converters: An artificial neural network approach," IEEE Transactions on Industrial Electronics, 66(11), pp.8870-8880, 2018.
- [10] Khezri, R., Oshnoei, A., Yazdani, A. and Mahmoudi, A., "Intelligent coordinators for automatic voltage regulator and power system stabiliser in a multi-machine power system," IET Generation, Transmission & Distribution, 14(23), pp.5480-5490, 2020.
- [11] Saeed, M.U., Sun, Z. and Elias, S., "Semi-active vibration control of building structure by Self Tuned Brain Emotional Learning Based Intelligent Controller," Journal of Building Engineering, 46, p.103664, 2022.
- [12] Yazdani, A.M., Mahmoudi, A., Movahed, M.A., Ghanooni, P., Mahmoudzadeh, S. and Buyamin, S., "Intelligent speed control of hybrid stepper motor considering model uncertainty using brain emotional learning," Canadian Journal of Electrical and Computer Engineering, 41(2), pp.95-104, 2018.
- [13] Hsu, C.F. and Lee, T.T., "Emotional fuzzy sliding-mode control for unknown nonlinear systems. International Journal of Fuzzy Systems," 19(3), pp.942-953, 2017.
- [14] Iranpour, E. and Sharifian, S., "An FPGA implemented brain emotional learning intelligent admission controller for SaaS cloud servers," Transactions of the Institute of Measurement and Control, 39(10), pp.1522-1536, 2017.
- [15] Qutubuddin, M. D., and Narri Yadaiah. "Modeling and implementation of brain emotional controller for permanent magnet synchronous motor drive," Engineering Applications of Artificial Intelligence 60, pp.193-203, 2017.
- [16] "IEC-International Electrotechnical Commission," IEC 62040-2, 2016.